Synthesis and Applications of a Novel Supramolecular Polymer Network with Multiple H-Bonded Melamine Pendants and Uracil Crosslinkers

Dhananjaya Patra,[1] Mohan Ramesh,[1] Duryodhan Sahu,[1] Harihara Padhy,[1] Chih-Wei Chu,[2,3] Kung-Hwa Wei,[1] Hong-Cheu Lin[1]

[1]Department of Materials Science and Engineering, National Chiao Tung University, Hsinchu, Taiwan, Republic of China
[2]Research Center for Applied Sciences, Academia Sinica, Taipei, Taiwan, Republic of China
[3]Department of Photonics, National Chiao Tung University, Hsinchu, Taiwan, Republic of China
Correspondence to: H.-C. Lin (E-mail: linhc@mail.nctu.edu.tw) and C.-W. Chu (E-mail: gchu@gate.sinica.edu.tw)

Received 1 September 2011; accepted 8 November 2011; published online 1 December 2011
DOI: 10.1002/pola.25853

ABSTRACT: A conjugated main-chain copolymer (**PBT**) consisting of bithiazole, dithieno[3,2-b:2′,3′-d]pyrroles (DTP), and pendent melamine units was synthesized by Stille polymerization, which can be hydrogen-bonded (H-bonded) with proper molar amounts of bi-functional π-conjugated crosslinker **F** (i.e., two uracil motifs covalently attached to a fluorene core through triple bonds symmetrically) to develop a novel supramolecular polymer network (**PBT/F**). The effects of multiple H-bonds on light harvesting capabilities, HOMO levels, and photovoltaic properties of polymer **PBT** and H-bonded polymer network **PBT/F** are investigated. The formation of supramolecular polymer network (**PBT/F**) between **PBT** and **F** was confirmed by FTIR and XRD measurements. Because of the stronger light absorption, lower HOMO level, and higher crystallinity of H-bonded polymer network **PBT/F**, the solar cell device containing **PBT/F** showed better photovoltaic properties than that containing polymer **PBT**. The preliminary results show that the solar cell device containing 1:1 weight ratio of **PBT/F** and [6,6]-phenyl C_{71} butyric acid methyl ester ($PC_{71}BM$) offers the best power conversion efficiency (PCE) value of 0.86% with a short-circuit current density (J_{sc}) of 4.97 mA/cm^2, an open circuit voltage (V_{oc}) of 0.55 V, and a fill factor (FF) of 31.5%. © 2011 Wiley Periodicals, Inc. J Polym Sci Part A: Polym Chem 50: 967–975, 2012

KEYWORDS: atomic force microscopy; H-bonded; polymer network; self-assembly; supramolecular structure

INTRODUCTION During the past decade, semiconducting polymers containing supramolecular structures, including hydrogen-bonds (H-bonds), are one of the key targets for sensors and optoelectronic devices.[1] Owing to the self-assembly behavior, high specificity, and directionality of H-bonds,[2] well-defined nanostructures and mesoscopic assemblies are generated by utilizing complementary hydrogen-bonding concept. Because of self-assembly between complementary molecular components, various kinds of noncovalent interactions, such as hydrogen-bonds (H-bonds),[3] ionic forces,[4] and metal-coordinations,[5] can give rise to unique properties, which are not possessed by their individual components. Extensive researches devoted towards engineering of polymeric materials as well as devices in electron donor–acceptor (D-A) bulk heterojunction (BHJ) solar cells due to the substantial future prospects of low-cost photovoltaic technologies.[6] Recently, power conversion efficiency (PCE) values have reached over 7% by an active layer of low-band-gap (LBG) electron-donating polymers and electron-accepting fullerene derivatives, such as [6,6]-phenyl-C_{61}-butyric acid methyl ester ($PC_{61}BM$) or [6,6]-phenyl-C_{71}-butyric acid methyl ester ($PC_{71}BM$).[7] A numerous advantages of LBG polymers, such as broad absorption spectra, fine controls of molecular energy levels, high mobilities, and favorable morphologies, were utilized for organic solar cells.[8] A solution processable dithieno[3,2-b: 2′,3′-d]pyrroles (DTP) unit, as an efficient electron-donating unit, can be copolymerized with various electron-deficient moieties to form LBG polymers possessing PCE values up to ~3%.[9] However, because of high values of highest occupied molecular orbital (HOMO) levels in DTP-based polymers, they showed relatively low V_{oc} values and thus to result in low PCE values for organic solar cells.[10] This problem can be solved by either using different electron-deficient units[9a,b] or introducing supramolecular architectures to manipulate their HOMO energy levels and thus to get higher V_{oc} values. The introduction of electron-deficient units, for example, bithiazole, could be one of the best choices as it showed high oxidative stabilities by lowering the HOMO level.[9a,b,11] Lately, we have introduced organic dyes (as proton donors) to be H-bonded with side-chain

Additional Supporting Information may be found in the online version of this article

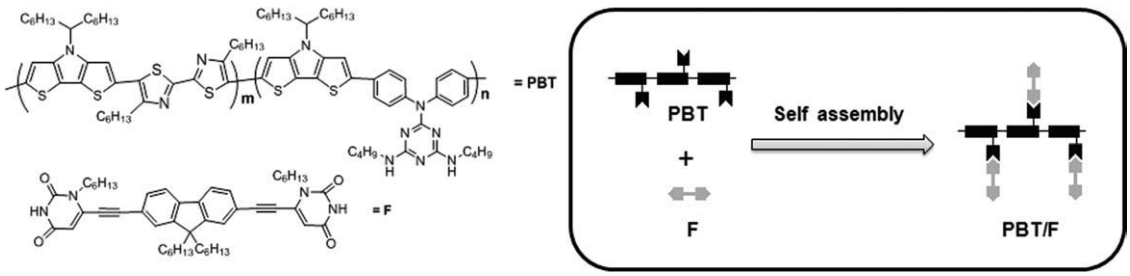

FIGURE 1 Schematic representation of **PBT/F** after complexation with **PBT** and **F**.

pyridyl polymers (as proton acceptors) for the application of BHJ solar cell devices, where the PCE values were mainly contributed from the organic dyes rather than the side-chain polymers.[3b,c]

Herein, we synthesized a conjugated main-chain copolymer (**PBT**) by introducing bithiazole, DTP, and pendent melamine units, and the supramolecular polymer network could be formed by mixing with stoichiometric amounts of **PBT** and bifunctional π-conjugated crosslinker (**F**), that is, **PBT**:**F** = 2:1 in molar ratio. As shown in Figure 1, two uracil motifs of **F** (as H-bonded crosslinking sites) attached to a fluorene core via triple bonds can be H-bonded with the complementary melamine pendants of the main-chain copolymer (**PBT**). To the best of our knowledge, the supramolecular polymer network (**PBT/F**) is first developed by H-bonded complexation of LBG main-chain copolymer **PBT** containing melamine pendants and π-conjugated crosslinker **F**. The unique features of this multiple H-bonding approach to optimizing light harvesting and manipulating HOMO level of polymer **PBT** by incorporating H-bonded crosslinker **F** through supramolecular architecture are investigated.

EXPERIMENTAL

Materials

All chemicals and solvents were reagent grades and purchased from Aldrich, ACROS, Fluka, TCI, TEDIA, and Lancaster Chemical Tetrahydrofuran (THF) and toluene, were distilled over sodium/benzophenone. Other reagents were used as received without further purification. Monomers **M2**,[11a] **M3**,[12] and 2,7-diethynyl-9,9-dihexyl-9*H*-fluorene[5a] were synthesized by our previously reported synthetic procedures.

Measurements and Characterization

^{1}H and ^{13}C NMR spectra were recorded on a Varian Unity 300 MHz spectrometer using $CDCl_3$ solvent and chemical shifts were reported as δ values (ppm) relative to an internal tetramethylsilane (TMS) standard. Elem. Anal. were performed on a HERAEUS CHN-OS RAPID elemental analyzer. Thermogravimetric analyses were conducted with a TA Instruments Q500 at a heating rate of 10 °C/min under nitrogen. Gel permeation chromatography (GPC) analyses were conducted on a Waters 1515 separation module using polystyrene as a standard and THF as an eluant. Fourier transform infrared (FTIR) spectra of samples (dispersed in KBr disks) were recorded on a Perkin-Elmer Spectrum 100 Series. UV–visible absorption spectra were recorded in dilute dichlorobenzene solutions on a HP G1103A spectrophotometer. Thin films of UV–vis measurements were spin-coated on glass substrates from dichlorobenzene solutions with a concentration of 5 mg/mL. Cyclic voltammetry (CV) measurements were performed by a scanning rate of 100 mV/s at room temperature using a BAS 100 electrochemical analyzer with a standard three-electrode electrochemical cell in a 0.1 M tetrabutylammonium hexafluorophsphate ($TBAPF_6$) solution in acetonitrile. During the CV measurements, the solutions were purged with nitrogen for 30 s. In each case, a carbon rod coated with a thin layer of polymers as the working electrode, a platinum wire as the counter electrode, and a silver wire as the quasi-reference electrode were used, and Ag/AgCl (3 M KCl) electrode was served as a reference electrode for all potentials quoted herein. The redox couple of ferrocene/ferocenium ion (Fc/Fc^+) was used as an external standard. The corresponding highest occupied molecular orbital (HOMO) and lowest unoccupied molecular orbital (LUMO) levels were calculated using E_{onset}^{ox} and E_{onset}^{red} for experiments in solid films of polymers, which were performed by drop-casting films with the similar thickness from THF solutions (ca. 5 mg/mL). The LUMO level of PCBM employed was in accordance with the literature datum. The onset potentials were determined from the intersections of two tangents drawn at the rising currents and background currents of the CV measurements. Topographic images of the copolymer: $PC_{61}BM$ or $PC_{71}BM$ films (surface area: 2 × 2 μm^2) were obtained through atomic force microscopy (AFM) in the tapping mode under ambient conditions using (AFM, Digital instrument NS 3a controller with D3100 stage). The small-angle X-ray diffraction (SAXD) measurements were performed at the beamline BL17A of the National Synchrotron Radiation Research Center (NSRRC), Taiwan.

Fabrication and Testing of Polymer Solar Cell Devices

The polymer photovoltaic (PV) cells in this study contained an active layer of [6,6]-phenyl-C_{61}-butyric acid methyl ester ($PC_{61}BM$) or [6,6]-phenyl-C_{71}-butyric acid methyl ester ($PC_{71}BM$) blended with polymer **PBT** and H-bonded polymer network **PBT/F**, respectively, in solid film, which was sandwiched between a transparent indium tin oxide (ITO) anode and a metal cathode (Ca). Prior to the device fabrication, ITO-coated glass substrates (1.5 × 1.5 cm^2) were ultrasonically cleaned in detergent, deionized water, acetone, and isopropyl alcohol. After routine solvent cleaning, the substrates

were treated with UV ozone for 20 min. Then, a modified ITO surface was obtained by spin-coating a layer of poly(ethylene dioxythiophene):polystyrenesulfonate (PEDOT:PSS) (~30 nm). After baking at 130 °C for 1 h, the substrates were transferred to a nitrogen-filled glove box. Subsequently, on the top of PEDOT:PSS layer, the active layer was prepared by spin-coating from blended solutions of polymers: $PC_{61}BM$ or $PC_{71}BM$ (1:1 w/w) with a spin rate about 1000 rpm, and the thickness of the active layer was typically about 90 nm. Initially, the blended solutions were prepared by dissolving both polymers and $PC_{61}BM$ or $PC_{71}BM$ in 1,2 dichlorobenzene (DCB)(10 mg/1 mL), followed by continuous stirring for 12 h at 50 °C. In the slow-growth approach, blended polymers in solid films were kept in the liquid phase after spin-coating by using the solvent DCB with a high boiling point. Finally, a calcium layer (30 nm) and a subsequent aluminum layer (100 nm) were thermally evaporated through a shadow mask at a pressure below 6×10^{-6} torr to have the active device area of 0.12 cm^2. All polymer solar cell (PSC) devices were annealed at 70 °C for 30 min. before measurements. The solar cell testing was done at room temperature inside a glove box under simulated AM 1.5G irradiation (100 mW/cm^2) using a Xenon lamp-based solar simulator (Thermal Oriel 1000W). The light intensity was calibrated by a mono-silicon photodiode with KG-5 color filter (Hamamatsu). The external quantum efficiency (EQE) action spectra were obtained at short-circuit conditions. The light source was a 450 W Xe lamp (Oriel Instrument, model 6266) equipped with a water-based IR filter (Oriel Instrument, model 6123NS). The light output from the monochromator (Oriel Instrument, model 74100) was focused on the photovoltaic cell under test.

Fabrication of Hole Only Devices

The hole devices[9b] in this study containing polymers **PBT** or **PBT/F**:$PC_{61}BM$ (1:1) blend film sandwiched between transparent ITO anode and cathode. The devices were prepared following the same procedure as fabrication of bulk-heterojunction (BHJ) devices, except that in the hole-only devices, Ca was replaced with MoO_3 ($\Phi = 5.3$ eV). The MoO_3 was thermally evaporated to a thickness of 20 nm and then capped with 50 nm of Al on the top of active layer. The devices, annealing of the active layer was performed at 130 °C for 20 min. The hole-mobilities were determined precisely by fitting the plot of the dark current versus the voltage (J–V) curves for single carrier devices to the SCLC model. The dark current is given by $J = 9\varepsilon_0\varepsilon_r\mu V^2/8L^3$, where $\varepsilon_0\varepsilon_r$ is the permittivity of the polymer, μ is the carrier mobility, and L is the device thickness.

Synthesis of Monomers and Polymers

4,6-Dichloro-N,N-diphenyl-1,3,5-triazin-2-amine (1)

Under N_2, a solution of diphenylamine (9.16 g, 54.22mmol) in THF (50 mL) was added dropwise to a mixture of diisopropylethylamine (9.5 mL, 54.22 mmol) and 2,4,6-trichloro-1,3,5-triazine (10.0 g, 52.22 mmol) in THF(150 mL) at 20 °C. After stirring for 3 h, the solvent was removed by rotatary evaporation and the residue was purified by column chromatography over silica gel (hexane: ethyl acetate = 4:1) to give a white color solid. (12.9 g, yield 75%).

^{1}H NMR (300 MHz, $CDCl_3$, δ):7.45–7.41 (m, 4H), 7.35–7.33 (m, 2H), 7.30–7.27 (m, 4H).

N^2,N^4-Dibutyl-N^6,N^6-diphenyl-1,3,5-triazine-2,4,6-triamine (2)

Sodium bicarbonate (8.0 g, 84.01 mmol) was added to a solution of compound 1 (10.0 g, 31.52 mmol) in 1,4-dioaxane (100 mL). After that, butyl amine (9.4 mL, 94.58 mmol) was added and the resulting mixture was refluxed for overnight. The reaction mixtures was cooled to room temperature and pour into cold water and extracted three times with ethyl acetate. The combined organic fractions were washed with brine, dried over $MgSO_4$, and concentrated by rotary evaporation and purified by column chromatography using silica, (hexane: ethyl acetate = 7:3) to give a white solid. (10.70 g, yield 87%).

^{1}H NMR (300 MHz, $CDCl_3$, δ):7.45–7.41 (m, 4H), 7.35–7.33 (m, 2H), 7.30–7.27 (m, 4H),4.84 (br, 2H), 3.34–3.11(br, 4H), 1.43–1.25 (m, 8H), 0.88 (t, $J = 6.2$Hz, 6H).

N^2,N^2-Bis(4-bromophenyl)-N^4,N^6-dibutyl-1,3,5-triazine-2,4,6-triamine (M1)

NBS (6.9 g, 38.40 mmol) was added portion-wise to a solution of compound **2** (5.0 g, 12.80 mmol) in DMF (50 mL) at 0 °C. The reaction mixture was stirred for 6 h at the same temperature and water was added to quench the reaction. The organic layer was extracted with three times by ethyl acetate followed by brine and water washing and dried by anhydrous $MgSO_4$. The solvent was removed by rotary evaporator and the product was further purified by column chromatography on silica (hexane: ethyl acetate = 4:1) to yield a white solid. (5.7 g, 80%).

^{1}H NMR (300 MHz, $CDCl_3$, δ):7.47–7.38 (m, 4H), 7.43–7.28 (m, 4H), 4.84 (br, 2H), 3.34–3.31(br, 4H), 1.43–1.25 (m, 8H), 0.88 (t, $J = 6.2$ Hz, 6H). ^{13}C NMR (75 MHz, $CDCl_3$, δ):166.48, 166.11, 143.25, 131.81, 129.77, 118.79, 40.60, 32.09, 20.24, 14.01; EIMS [M^+] calcd. $m/z = 548.32$, found 548.0. Anal. Calcd. for $C_{23}H_{28}Br_2N_6$: C, 50.38; H, 5.15; Br, 29.15; N, 15.33; found: C, 50.78; H, 5.48; N, 15.04.

1-Hexyluracil (3)

K_2CO_3 (14.80 g, 107.05 mmol) was added to a suspension of uracil (10.0 g, 89.21 mmol) in DMSO (150 mL), and stirred for 15–20 min at 45 °C. 1-Bromohexane (3.5 mL, 25 mmol) was added and the reaction mixture was stirred for 48 h. The reaction was cooled to room temperature and poured into cold water. The product was extracted three times with DCM, and washed with dilute HCl, water, brine, and dried over $MgSO_4$. The organic layer was concentrated and poured into cold hexane with vigorous stirring. The resulting precipitate was filtered and washed with cold hexane to afford compound **3** (12.40 g, 70.9%) as a white solid.

^{1}H NMR (300 MHz, $CDCl_3$, δ):9.12 (br, 1H), 7.14 (d, $J = 9.0$ Hz, 1H), 5.70 (d, $J = 6.0$ Hz, 1H), 3.71(t, $J = 7.5$ Hz, 2H),

1.74–1.65 (m, 2H), 1.34–1.27 (m, 6H), 0.88 (t, J = 6.6 Hz, 3H).

1-Hexyl-6-iodouracil (4)

At −78 °C, LDA (20.4 mL of a 2.5 M solution, 51.0 mmol) was added drop-wise to a solution of 1-hexyluracil (2.0 g, 10.2 mmol) in THF (55 mL), and the resulting solution was stirred under N_2 for 2 h. I_2 (12.9 g, 51.0 mmol) was added and the reaction mixture was stirred for another 2 hr at the same temperature. Acetic acid (2.0 mL) was added to react with stirring at room temperature for overnight. The organic phase was extracted with ethyl acetate washed with saturated $NaHCO_3$ (3 × 30.0 mL) and Na_2SO_3 (3 × 30 mL) solutions. Finally, the product was washed with brine (30 mL), and dried over Mg_2SO_4. The solvent was removed by rotary evaporator and the crude product was purified by column chromatography silica (hexane: ethyl acetate = 5:5) to afford compound **4** (2.2 g, 67%).

^{1}H NMR (300 MHz, $CDCl_3$, δ):9.48 (br, 1H), 6.41 (s, 1H), 4.0 (t, J = 8.1 Hz, 2H), 1.74–1.65 (m, 2H), 1.34–1.27 (m, 6H), 0.88 (t, J = 6.9 Hz, 3H).

6,6′-(9,9-Dihexyl-9H-fluorene-2,7-diyl)bis(ethyne-2,1-diyl)-bis(1-hexylpyrimidine-2,4(1H,3H)-dione) (F)

To a mixture of compound **4** (1.26 g, 3.9 mmol) in THF (15 mL), 2,7-diethynyl-9,9-dihexyl-9*H*-fluorene[3] (0.5 g, 1.3 mmol), triphenylphosphine(10 mg, 0.05), CuI (10 mg, 0.05 mmol), and NEt_3 (15 mL) were added. Then, $[Pd(PPh_2)Cl_2]$ (4 mg, 0.034mmol) was added under N_2 and the reaction mixture was heated to 50 °C for 36 h. The crude product was extracted with DCM followed by brine wash and dried over $MgSO_4$. The resulting solution was concentrated by rotary evaporator, and purified by column chromatography using silica, (hexane: ethyl acetate 7:3) to give a yellow solid. (0.58 g, yield 58%).

^{1}H NMR (300 MHz, $CDCl_3$, δ):9.60 (br, 2H), 7.77 (d, J = 8.1 Hz, 2H), 7.53 (m, 4H), 6.04 (m, 2H) 4.01 (t, J = 7.8 Hz, 4H), 2.0 (t, J = 8.1 Hz, 4H), 1.82 (t, J = 7.2 Hz, 4H), 1.44–1.34 (m, 12H), 1.36–1.08 (m, 12H), 1.15–1.08 (m, 12H), 0.88 (t, J = 6.9 Hz, 6H), 0.77 (t, J = 7.2, 6H), 0.59 (m, 4H). ^{13}C NMR (75 MHz, $CDCl_3$, δ): 162.96, 151.95, 151.08, 142.41, 138.89, 131.72, 126.58, 121.05, 119.76, 106.89, 101.28, 81.30, 55.84, 46.94, 40.31, 31.67, 29.77, 29.02, 26.65, 23.97, 22.77, 22.75, 14.19; EIMS [M^+] calcd. m/z = 771.04, found 772.0. Anal. Calcd. For $C_{49}H_{62}N_4O_4$: C, 76.33; H, 8.10; N, 7.27; O, 8.30; found: C, 76.00; H, 7.97; N, 7.17.

Synthesis of PBT via Stille Coupling Polymerization

Into 25 mL of two-neck flask, 1 equiv of dibromo monomers (**M1** and **M3**) and 2 equiv of 2,6-bis(tributylstannyl)-4-(tridecan-7-yl)-4*H*-dithieno[3,2-b: 2′,3′-d]pyrrole (**M2**) were added in anhydrous toluene and deoxygenated with nitrogen for 30 min. The Pd(0) complex, that is, tetrakis(triphenylphosphine)palladium (1 mol %), was transferred into the mixture in a dry environment. The reaction mixture was stirred at 110 °C for 48 h, and then an excess amount of 2-bromothiophene was added to end-cap the trimethylstannyl groups for 4 h. After cooling to room temperature, the solution was added dropwise into MeOH (200 mL). The crude polymer was collected, dissolved in hot $CHCl_3$, filtered through a 0.5-μm poly(tetrafluoroethylene) (PTFE) filter, and reprecipitated in MeOH. The solid was washed with acetone, hexane, and $CHCl_3$ in a Soxhlet apparatus. The $CHCl_3$ solution was concentrated and then added dropwise into MeOH. Finally, the polymer was collected and dried under vacuum to give **PBT**. Yield: 59%.

^{1}H NMR (300 MHz, $CDCl_3$, δ):7.53 (br), 7.45–7.04 (br), 4.90–4.65 (br), 4.15 (br), 3.36–2.97 (br), 2.10–1.60 (m), 1.55–0.90 (m), 0.87–0.65 (m). Anal. Calcd. For $C_{83}H_{114}N_{10}S_6$: C, 69.02; H, 7.96; N, 9.70; S, 13.32; Found: C, 68.31; H, 6.94; N, 10.41.

Preparation of Supramolecular Polymer Network

Supramolecular polymer (**PBT/F**) was prepared by dissolving 2 M of polymer **PBT** and 1 M bifunctional H-bonded π-conjugated crosslinker (**F**) in a minimum amount of $CHCl_3$ and then the solvent was evaporated under ambient temperature.

RESULTS AND DISCUSSION

Syntheses and Characterization

The synthetic details of monomers **M1**, H-bonded π-conjugated crosslinker **F**, and polymer **PBT** are depicted in Scheme 1, and their NMR spectra are illustrated in Supporting Information Figures S1–S3. **PBT** was synthesized by Stille copolymerization of three monomers **M1**, **M2**, and **M3** (1:2:1 in molar ratio), and **F** was synthesized by sonogashira coupling of 2,7-diethynyl-9,9-dihexyl-9*H*-fluorene and 1-hexyl-6-iodopyrimidine-2,4(1*H*,3*H*)-dione. According to the GPC result, **PBT** showed a number-average molecular weight (M_n) of 20.1 kg/mol with a polydisperse index (PDI) value of 1.43. The thermal stabilities of polymer **PBT** and H-bonded polymer network **PBT/F** were investigated by thermogravimetric analyses (TGA), and demonstrated in Figure 2. Both polymer **PBT** and H-bonded polymer network **PBT/F** showed good thermal stabilities and exhibited T_d values (temperatures at 5% weight loss by a heating rate of 10 °C/min under nitrogen) at 361 and 452 °C, which indicates that due to H-bonded effects the T_d value of H-bonded polymer network **PBT/F** is higher than that of polymer **PBT**. However, the crosslinker **F** in H-bonded polymer network **PBT/F** will be decomposed more completely at the final stage, so the final weight loss of H-bonded polymer network **PBT/F** (with a lower weight ratio of **PBT** to be sustained at the high temperature end) is larger than that of polymer **PBT**.

As shown in Figure 3, **F** demonstrates free C═O and N—H stretching bands located at 1,702 and 3,145 cm^{-1} and **PBT** demonstrates a N—H stretching band located at 3,278 cm^{-1} in their IR spectra.[13,14] After the formation of triple hydrogen bonds in H-bonded polymer network **PBT/F**, the C═O stretching band shifted to a lower wave number 1,687 cm^{-1} due to uracilic (C═O) vibrations with major contributions from N—H in plane bending modes[13] and NH—N stretching to a higher wave number at 3,302 cm^{-1}.[14] To gain insight into the structural orders of both polymers, powder X-ray diffraction (XRD) patterns of **PBT** and **PBT/F** were performed and demonstrated in Supporting Information Figure

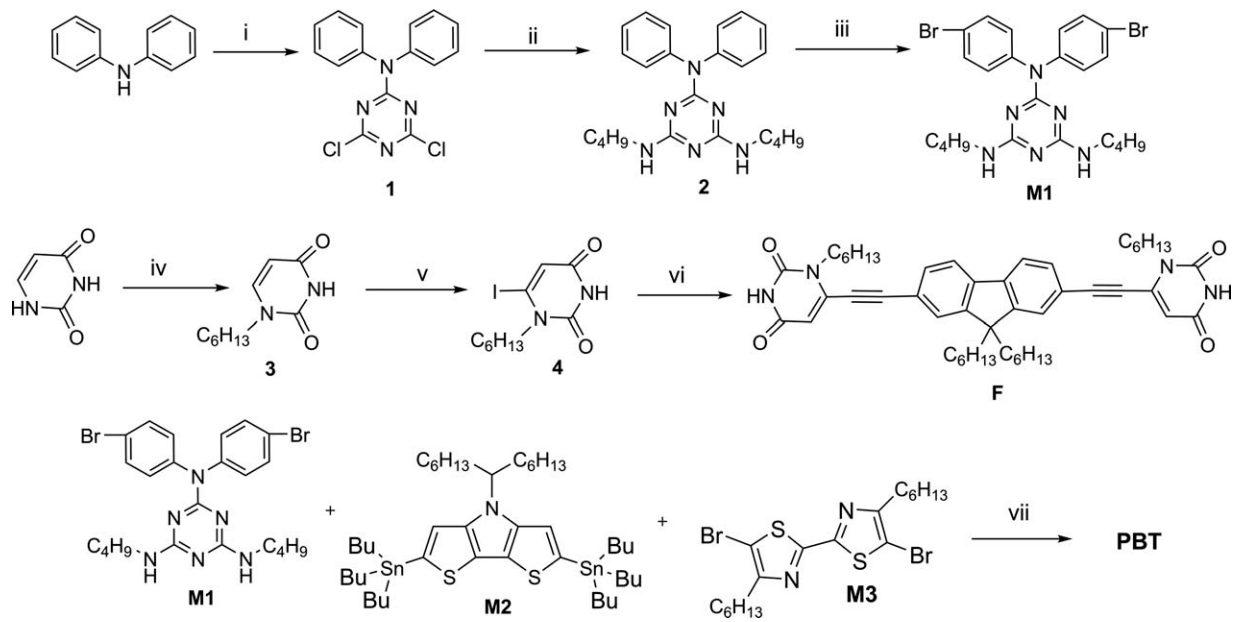

SCHEME 1 Synthetic Routes of **M1**, **F**, and Polymer **PBT**[a]. [a]Reagents and conditions: (i) diisopropylethylamine, THF, 20 °C, 3 h; (ii) sodium bicarbonate, 1,4-dioxane, reflux, overnight; (iii) NBS, 0–5 °C, THF; (iv) K_2CO_3, DMSO, 45 °C, overnight; (v) −78 °C, LDA, THF, 5 h, I_2;$Pd(PPh_3)_4$, toluene, 110 °C, 48 h; (vi) Ph_3P, CuI, THF, Et_3N, $Pd(PPh_2)Cl_2$, 50 °C, overnight; (vii) Toluene, $Pd(PPh_3)_4$, 110 °C, 48 h.

S4. It can be seen that **PBT/F** showed two more obvious XRD peaks than **PBT**, which indicates the higher crystallinity in H-bonded polymer network **PBT/F**.[5b] In contrast to **PBT**, the higher crystallinities in both small- and wide-angle regions of **PBT/F** are assumed to be increased by the presence of multiple hydrogen-bonds, which enhances chain-reorganization and self-assembled behavior and also induce a higher power conversion efficiency of H-bonded polymer network **PBT/F**.[1a]

Optical Properties

Figure 4 displays the absorption spectra of **PBT**, **PBT/F**, and **F**, measured from dichlorobenzene solutions (**PBT** and **F**) and solid films (**PBT**, **PBT/F**, and **F**), and their photophysical data are summarized in Table 1. The absorption maximum of **PBT** solution (in dichlorobenzene) was found to be 505 nm which can be attributed to intramolecular charge transfer between the electron donor (DTP) and acceptor (bithiazole) units.[11] Relative to the solution absorption, the absorption maximum is located at 520 nm in the solid film which is slightly red-shifted, indicating intermolecular interactions and aggregations occurred in solid films.[10c,11a] The absorption maximum of π-conjugated crosslinker **F** was found to be

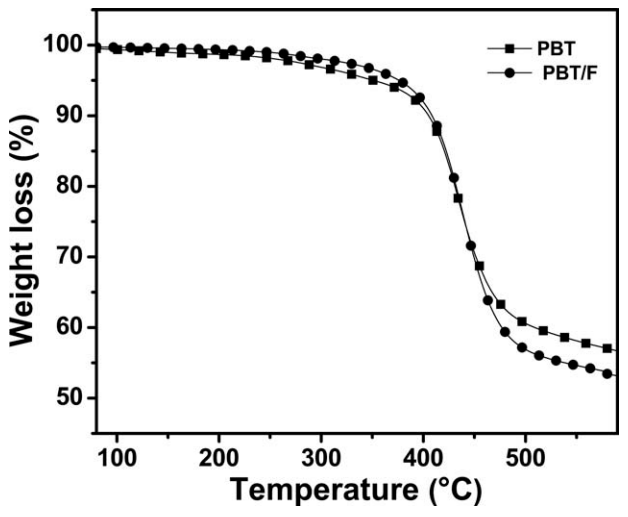

FIGURE 2 TGA thermogram of **PBT** and **PBT/F**, recorded at a heating rate of 10 °C min^{-1} under N_2 atmosphere.

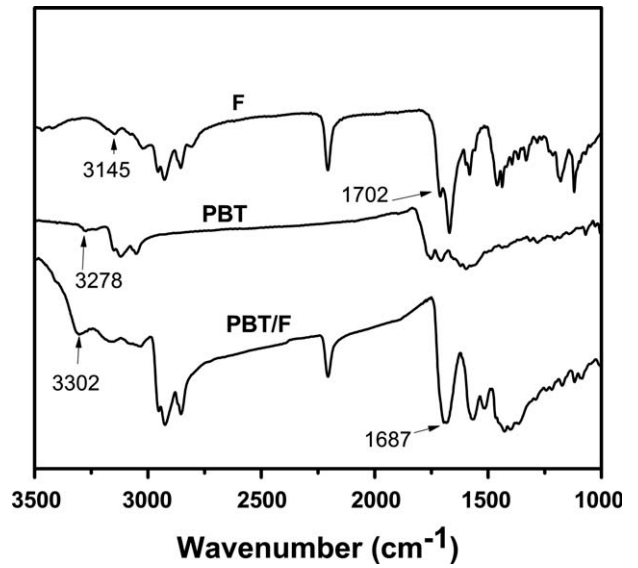

FIGURE 3 FTIR spectra of π-conjugated crosslinker **F**, polymer **PBT**, and supramolecular polymer network **PBT/F** at room temperature.

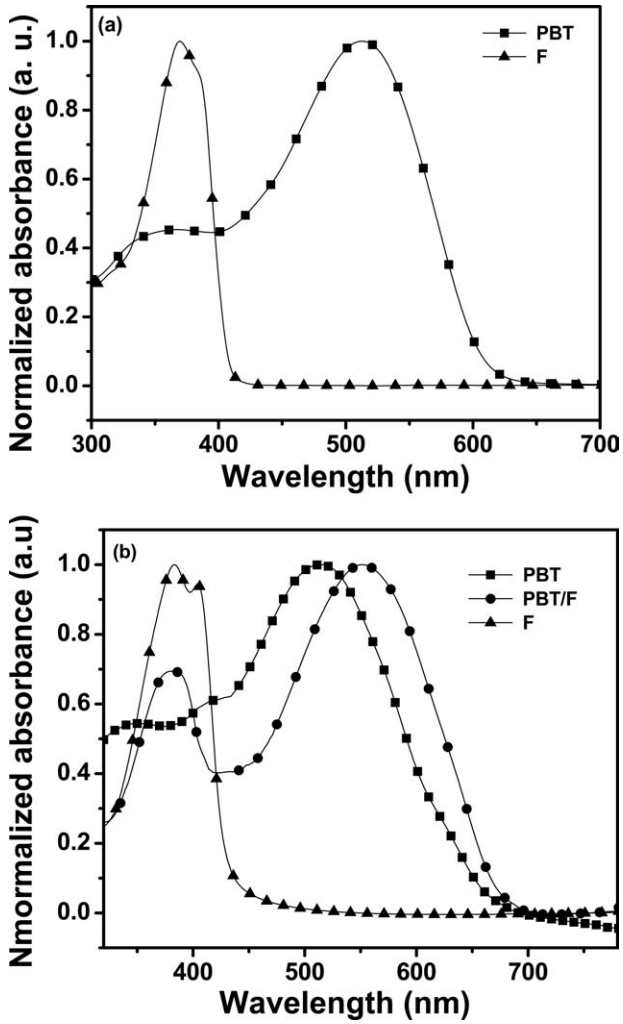

FIGURE 4 Normalized UV–Vis absorption spectra of (a) **PBT** and H-bonded π-conjugated crosslinker F in dilute dichlorobenzene solutions; and (b) **PBT**, **PBT/F**, and **F** in solid films.

369 nm (in the dichlorobenzene solution) and found to be 409 nm (in the solid film), respectively, where the red-shift of 40 nm in the solid film is due to the interchain association and π–π stacking of π-conjugated crosslinker **F**.[8c,15] Compared with **PBT** (in solid films), a new peak appeared at 385 nm in the UV region of H-bonded polymer network **PBT/F** by the introduction of **F**, and a red-shifted (ca. 28 nm, from 520 to 548 nm) absorption peak occurred due to the multiple H-bonded effect.[14b] The optical band-gaps (E_g^{opt}) of **PBT** and **PBT/F** were found from the cut-offs of the absorption wavelengths to be 1.80 and 1.77 eV, respectively. This result implies that it is an efficient way to tune optical properties of the side-chain polymer through supramolecular intractions to absorb maximum photons from visible regions for enhanced photovoltaic applications. Moreover, the homogeneous incorporation of the organic dye (a small molecule) to the polymer with a complimentary absorption band through multi-H-bonds so as to broaden the total light absorption (as shown in Fig. 4) and thus to induce enhanced photovoltaic properties, which can be further proven by PCE values and EQE measurements in later discussion.

Electrochemical Properties

Cyclic voltammetry (CV) measurements were employed to estimate the highest occupied molecular orbital (HOMO) and lowest unoccupied molecular orbital (LUMO) levels of polymers **PBT** and **PBT/F** and their CV curves are provided in Supporting Information Figure S5. The CV measurements were carried out in a 0.1 M tetrabutylammonium hexafluorophosphate (TBAPF6) solution (in acetonitrile) at a scan rate of 100 mV/s under nitrogen. A carbon electrode, which was coated with the polymer film by dip coating, was used as a working electrode and Ag/AgCl was served as a reference electrode, and it was calibrated by ferrocene ($E^{1/2}_{ferrocene}$ = 0.45 mV vs. Ag/AgCl). The HOMO and LUMO energy levels were estimated by the oxidation and reduction potentials from the reference energy level of ferrocene (4.8 eV below the vacuum level) according to the following equation[16] : $E_{HOMO/ELUMO} = [-(E_{onset} - E_{onset\ (FC/FC^+\ vs.\ Ag/Ag^+)}) - 4.8]$ eV and band gap = $E^{ox}_{onset} - E^{red}_{onset}$ (where 4.8 eV is the energy level of ferrocene below the vacuum level and $E_{onset\ (FC/FC^+\ vs.\ Ag/Ag^+)} = 0.45$ eV). The HOMO and LUMO levels as well as the electrochemical band-gap (E^{ec}_g) were determined from oxidation and reduction potentials (E^{ox}_{onset} and E^{red}_{onset}) of both polymers and their values are summarized in Table 1. It can be seen that polymer **PBT**, crosslinker **F**, and H-bonded polymer network **PBT/F** possess both quasi-irreversible p-doping/dedoping (oxidation/rereduction) processes at positive potentials and n-doping/dedoping (reduction/reoxidation) processes at negative potentials.

The onset potentials of (oxidation; reduction) of polymer **PBT**, crosslinker **F**, and those of H-bonded polymer network

TABLE 1 Optical and Electrochemical Properties of **PBT** and **PBT/F**

Polymer	Solution[a] λ_{abs} (nm)	Solid Film[b] λ_{abs} (nm)	E^{ox}_{onset} (V)/ HOMO[c] (eV)	E^{red}_{onset} (V)/ LUMO[c] (eV)	E^{opt}_g/E^{ec}_g (eV)
PBT	505	520	0.77/−5.12	−0.84/−3.51	1.80/1.61
F	369	409	1.49/−5.84	−1.11/−3.24	2.66/2.60
PBT/F	–	385, 548	0.89/−5.24	−0.91/−3.44	1.77/1.80

[a] In dilute dichlorobenzene solution.
[b] Spin coated from dilute dichlorobenzene solution on glass surface.
[c] HOMO/LUMO = $[-(E_{onset} - E_{onset(FC/FC^+\ vs.\ Ag/Ag^+)}) - 4.8]$ eV where 4.8 eV is the energy level of ferrocene below the vacuum level and $E_{onset\ (FC/FC^+\ vs.\ Ag/Ag^+)} = 0.45$ eV.

TABLE 2 Photovoltaic Properties[a] and Film Roughnesses[b] (R_{rms} measured by AFM) of Bulk-Heterojunction PSC Devices Containing **PBT** and **PBT/F** with $PC_{61}BM$ and $PC_{71}BM$ in a blending weight ratio of 1:1

Active layer (1:1 by wt.)	V_{oc} (V)	J_{sc} (mA/cm^2)	FF (%)	PCE (%)	R_{rms} (nm)
PBT:$PC_{61}BM$	0.50	2.07	33.0	0.34	1.46
PBT/F:$PC_{61}BM$	0.55	3.60	35.4	0.70	0.52
PBT:$PC_{71}BM$	0.50	2.90	39.3	0.57	0.50
PBT/F:$PC_{71}BM$	0.55	4.97	31.5	0.86	0.42

[a] Measured under AM 1.5 irradiation, 100 mW/cm^2.
[b] R_{rms}: root-mean-square values of roughness measured by AFM.

PBT/F, were found to be (0.77; −0.84) V, and (1.49; −1.11), and (0.89; −0.91) V, respectively. The estimated values of (HOMO; LUMO) levels for polymer **PBT**, crosslinker **F**, and those of H-bonded polymer network **PBT/F** were found to be (−5.12; −3.51) eV, (−5.84; −3.84), and (−5.24; −3.44) eV, respectively. Compared with polymer **PBT**, the lower HOMO level of H-bonded polymer network **PBT/F** (induced by the H-bonded structure) indicates that it could be more stable against oxidation due to the incorporation of highly oxidative stable fluorene in crosslinker **F**.[17,18] Compared with polymer **PBT**, the lower HOMO energy level of H-bonded polymer network **PBT/F** (as a donor material) is desirable for the high open circuit voltage of PSC.[18] The LUMO energy levels of the electron donors (**PBT** and **PBT/F**) have to be positioned above the LUMO energy levels of the acceptors (e.g., PCBM) at least 0.3 eV, so the exciton binding energy of polymer could be overcome and result in efficient electron transfer from donors to acceptors.

Photovoltaic Properties

PBT and **PBT/F** were utilized as electron donors to investigate the photovoltaic properties of BHJ photovoltaic devices with a device structure of ITO/PEDOT-PSS/polymers:acceptors/Ca/Al, where $PC_{61}BM$ (or $PC_{71}BM$) was an electron acceptors. Table 2 and Figure 5 demonstrate current density-voltage (*J-V*) curves of **PBT** and **PBT/F** blended with $PC_{61}BM$ (or $PC_{71}BM$) with a weight ratio of 1:1. (The photovoltaic devices with thicknesses ca. 90 nm were annealed at 70 °C and tested under 100 mW/cm^2 AM 1.5G solar illumination condition.) It can be clearly seen that H-bonded polymer network **PBT/F** possessed higher PCE values than polymer **PBT**. However, Li et al. have reported an analogous D-A copolymer containing DTP and bithiazole moieties only possessed V_{oc} = 0.28 V, J_{sc} = 0.51 mA/cm^2, and a maximum PCE value of 0.06%.[10c] In addition, recently we reported a similar polymer with a PCE of 0.27%.[9b] The most efficient solar cell device exhibited a PCE of 0.86% with V_{oc}, J_{sc}, and FF (fill factor) values 0.55 V, 4.97 mA/cm^2, and 31.5%, respectively. Compared with **PBT**, the higher PCE value of 0.86% in H-bonded polymer network **PBT/F** was improved by larger V_{oc} and J_{sc} values were due to a lower value of HOMO energy level (to induce a larger V_{oc} value), a higher light harvesting amount (by introducing **F** to induce a larger J_{sc} value) in visible regions, and an improved crystallinity (by introducing **F** to have a higher crystallinity). For effective charge carrier transport, hole-mobility is a key parameter and also equally affects FF values of the solar cell devices.[8d] We employed hole-only devices to characterize the hole mobilities of **PBT** and **PBT/F** films blended with $PC_{61}BM$ and found to be 1.72 × 10^{-7} and 2.32 × 10^{-6} cm^2/Vs, respectively, and thus the low hole-mobilities of both polymers induced low FF values (<40%, see Table 2).[8d]

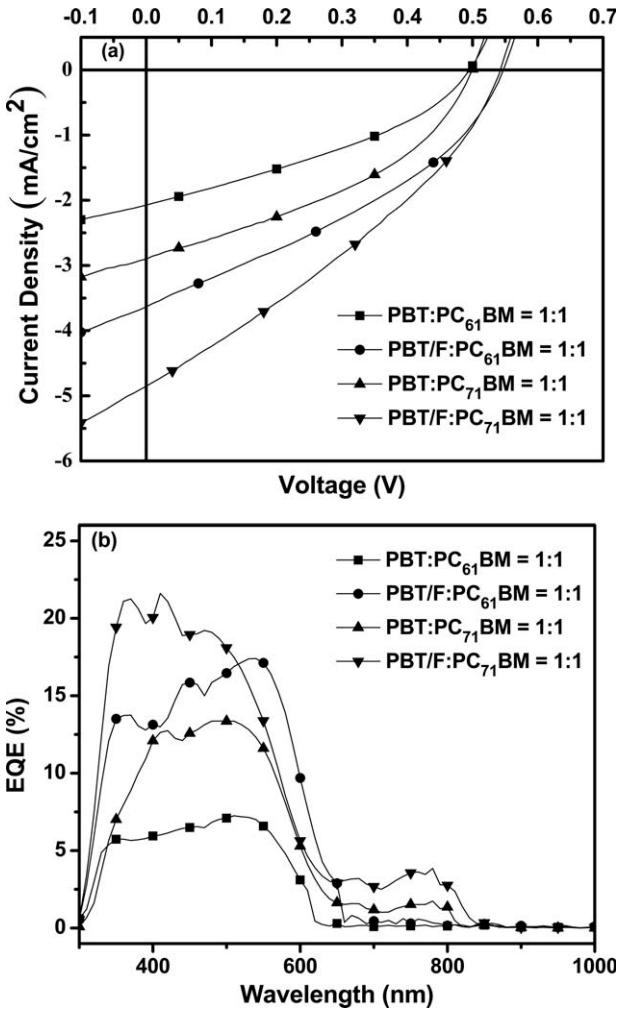

FIGURE 5 (a) *J*−*V* and (b) EQE characteristic curves of polymer **PBT** and H-bonded polymer network **PBT/F** blended with $PC_{61}BM$ (or $PC_{71}BM$) in a weight ratio of 1:1.

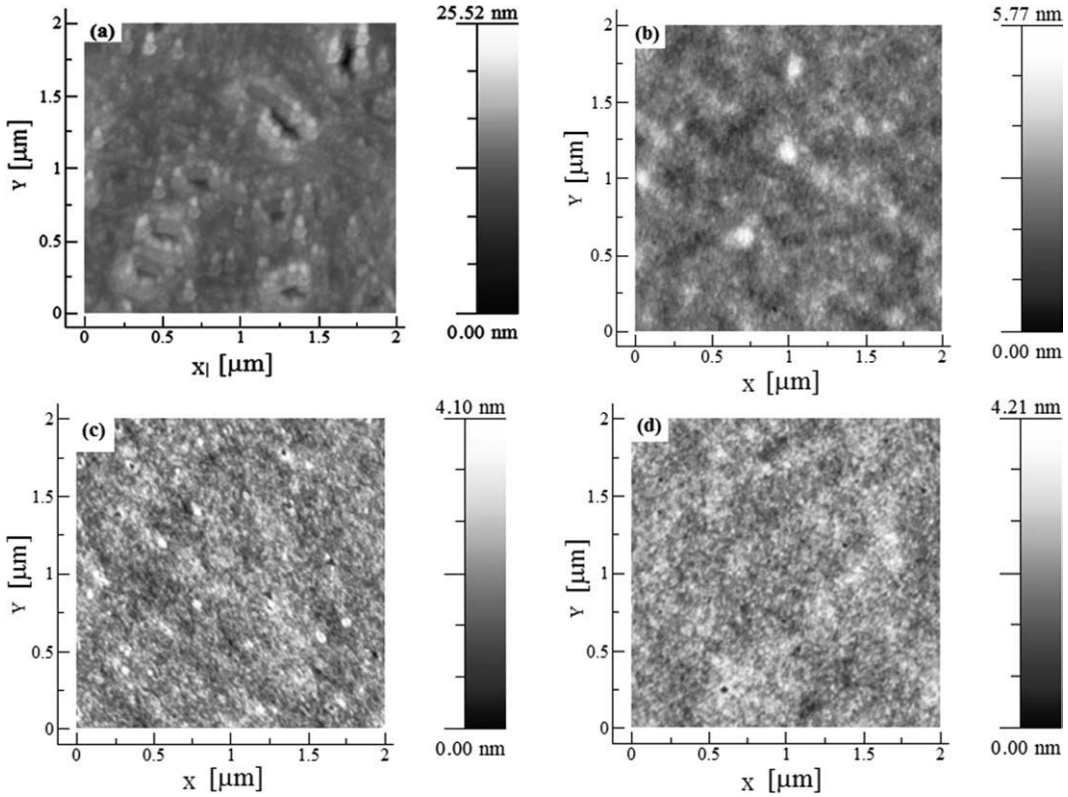

FIGURE 6 AFM images of blended polymers (a) **PBT** and (b) **PBT/F** mixed with $PC_{61}BM$, respectively; (c) **PBT** and (d) **PBT/F** mixed with $PC_{71}BM$, respectively (in a weight ratio of 1:1 by spin-coating from dichlorobenzene and annealing at 70 °C for 30 min).

In order to understand the origins of low current densities, we carried out external quantum efficiency (EQE) measurements for solar cell devices by mixing either $PC_{61}BM$ or $PC_{71}BM$ with polymers **PBT** and **PBT/F** (1:1 by wt.), respectively (Fig. 5). The results illustrate the solar cell devices containing H-bonded polymer network **PBT/F** are able to have higher absorptions of visible lights, which demonstrates enhancements of EQE values with a maximum of ~20% (ca. 350–550 nm) after incorporation of **F** with **PBT** through supramolecular interactions. Hence, the lower current densities of solar cell devices containing **PBT** (without **F**) might be induced by their smaller EQE values and lower hole-mobilities.[19]

Surface morphologies of the active layer in solar cell devices are also a key parameter for the device performance.[20] AFM images of blended polymers **PBT** and **PBT/F** mixed with either $PC_{61}BM$ or $PC_{71}BM$ (1:1 by wt. and annealed at 70 °C for 30 min) are presented in Figure 6 and their root-mean-square roughness (R_{rms}) values are demonstrated in Table 2. The active layers of **PBT** and **PBT/F** showed good film formation to have smooth surfaces with no obvious aggregations (only nano-scale phase separations) between polymers and $PC_{61}BM$ (or $PC_{71}BM$).[18] Mixed with $PC_{61}BM$ (or $PC_{71}BM$) in a weight ratio of 1:1, **PBT** (without **F**) showed larger R_{rms} values than H-bonded polymer network **PBT/F** in the blended polymers. This larger R_{rms} value resulted in the decreased diffusional escape probabilities for mobile charge carriers, and hence increased their recombinations.[20] It is evident from AFM images that lesser aggregation between electron-donor polymer and electron-acceptor PCBM molecules and higher π–π stacking allows for better photogenerated charges and inducing higher J_{sc} values via supramolecular engineering of solar cell devices.[20a]

CONCLUSION

In conclusion, we could tune molecular energy levels, morphologies, and device performances by a new and straightforward approach to introducing multiple H-bonded supramolecular structures. The broader light absorption (an extra blue absorption from H-bonded crosslinker **F** and the red-shifted absorption from H-bonded main-chain polymer **PBT**), lower HOMO level (to have a higher V_{oc} value), higher hole mobility, larger crystallinity, and better morphology in H-bonded polymer network **PBT/F** induces better photovoltaic properties than that containing polymer **PBT**. The preliminary photovoltaic performance showed the solar cell device containing 1:1 weight ratio of **PBT/F** and [6,6]-phenyl C_{71} butyric acid methyl ester ($PC_{71}BM$) offers the best power conversion efficiency (PCE) value of 0.86% with a short-circuit current density (J_{sc}) of 4.97 mA/cm^2, an open circuit voltage (V_{oc}) of 0.55 V, and a fill factor (FF) of 31.5%. The highly directional multiple H-bonded strategy between melamine and uracil motifs significantly increased self-assembled behavior as well as π–π stackings, which is an encouraging

method for the future researches to adjust the photovoltaic properties of polymer solar cell devices.

The financial supports of this project provided by the National Science Council of Taiwan (ROC) through NSC 97-2113-M-009-006-MY2 and National Chiao Tung University through 97W807 are acknowledged.

REFERENCES AND NOTES

1 (a) Greef, T. F. A. D.; Smulders, M. M. J.; Wolffs, M.; Schenning, A. P. H. J.; Sijbesma, R. P.; Meijer, E. W. *Chem. Rev.* **2009,** *109*, 5687–5754; (b) González-Rodriáguez, D.; Schenning, A. P. H. *J. Chem. Mater.* **2011,** *23*, 310–325.

2 (a) Pollino, J. M.; Weck, M. *Chem. Soc. Rev.* **2005,** *34*, 193; (b) Hoeben, F. J. M.; Zhang, J.; Lee, C. C.; Pouderoijen, M. J.; Wolffs, M.; Würthner, F.; Schenning, A. P. H. J.; Meijer, E. W.; Feyter, S. D. *Chem. Eur. J.* **2008,** *14*, 8579−8589; (c) Shunmugam, R.; Gabriel, G. J.; Amaer, K. A.; Tew, G. N. *Macromol. Rapid. Commun.* **2010,** *31*, 784–793.

3 (a) Jonkheijm, P.; Stutzmann, N.; Chen, Z.; Leeuw, D. M.; Meijer, E. W.; Schenning, A. P. H. J.; Würthner, F. *J. Am. Chem. Soc.* **2006,** *128*, 9535–9540; (b) Liang, T. C.; Chiang, I. H.; Yang, P. J.; Kekuda, D.; Chu, C. W.; Lin, H. C. *J. Polym. Sci. Part A: Polym. Chem.* **2009,** *47*, 5998−6013; (c) Sahu, D.; Padhy, H.; Patra, D.; Kekuda, D.; Chu, C. W.; Chiang, I. H.; Lin, H. C. *Polymer* **2010,** *51*, 6182−6192; (d) Feldman, K. E.; Kade, M. J.; Greef, T. F. A. E.; Meijer, E. W.; Kramer, E. J.; Hawker, C. J. *Macromolecules* **2008,** *41*, 4694–4700.

4 (a) Macro, F.; Elisabetta, E.; Massimiliano, B.; Antonio, F.; Andrea, P.; Francesco, C. *J. Polym. Sci. Part A: Polym. Chem.* **2011,** *49*, 3437−3447; (b) Kozo M.; Takeshi E. *J. Polym. Sci. Part A: Polym. Chem.* **2011,** *49*, 3582−3587.

5 (a) Chen, Y. Y.; Tao, Y. T.; Lin, H. C. *Macromolecules* **2006,** *39*, 8559–8566; (b) Padhy, H.; Sahu, D.; Chiang, I. H.; Patra, D.; Kekuda, D.; Chu, C. W.; Lin, H. C. *J Mater Chem* **2011,** *21*, 1196–1205.

6 (a) Gendron, D.; Leclerc, M. *Energy Environ. Sci.* **2011,** *4*, 1225–1237; (b) Zhan X.; Zhu, D. *Polym. Chem.* **2010,** *1*, 409–419.

7 (a) Zhou, H.; Yang, L.; Stuart, A. C.; Price, S. C.; Liu, S.; You, W. *Angew Chem. In. Ed.* **2011,** *50*, 2995–2998; (b) Chu, T. Y.; Lu, J.; Beaupré, S.; Zhang, Y.; Pouliot, J. R.; Wakim, S.; Zhou, J.; Leclerc, M.; Li, Z.; Ding, J.; Tao, Y. *J. Am. Chem. Soc.* **2011,** *133*, 4250–4253.

8 (a) Song, S.; Kim, G. H.; Kang, I.; Jin, Y.; Kim, I.; Kim, J. Y.; Suh, H. *J. Polym. Sci. Part A: Polym. Chem.* **2011,** *49*, 3751−3758; (b) Song, S.; Jin, Y.; Park, S. H.; Cho, S.; Kim, I.; Lee, K.; Heeger.A. J.; Suh, H. *J. Mater. Chem.* **2010,** *20*, 6517–6523; (c) Chen, G. Y.; Cheng, Y. H.; Chou, Y. J.; Su, M. S.; Chen, C. M.; Wei, K. H. *Chem. Commun.* **2011,** 5064–5066; (d) Chen, Y. C.; Yu, C. Y.; Fan, Y. L.; Hung, L. I.; Chen, C. P.; Ting, C. *Chem. Commun.* **2010,** 6503–6505.

9 (a) Zhou, E.; Cong, J.; Tajima, K.; Yang, C.; Hashimoto, K. *Macromol. Chem. Phys.* **2011,** *212*, 305–310; (b) Patra, D.; Sahu, D.; Padhy, H.; Kekuda, D.; Chu, C. W.; Wei, K. H.; Lin, H. C. *Macromol. Chem. Phys.* **2011,** *212*, 1960–1970; (c) Yue, W.; Zhao, Y.; Shao, S.; Tian, H.; Xie, Z.; Geng, Y.; Wang, F. *J. Mater. Chem.* **2009,** *19*, 2199–2206.

10 (a) Zhou, E.; Cong, J.; Tajima, K.; Hashimoto, K. *Chem. Mater.* **2010,** *22*, 4890–4895; (b) Zhou, E.; Wei, Q.; Yamakawa, S.; Zhang, Y.; Tajima, K.; Yang, C.; Hashimoto, K. *Macromolecules* **2010,** *43*, 821–826; (c) Zhang, M.; Fan, H.; Guo, X.; He, Y.; Zhang, Z.; Min, J.; Zhang, J.Zhao, G.; Zhan, X.; Li, Y. *Macromolecules* **2010,** *43*, 5706–5712.

11 (a) Patra, D.; Sahu, D.; Padhy, H.; Kekuda, D.; Chu, C. W.; Lin, H. C. *J. Polym. Sci. Part A: Polym. Chem.* **2010,** *48*, 5479–5489; (b) Jung, I. H.; Yu, J.; Jeong, E.; Kwon, S.; Kong, H.; Lee, K.; Woo, H.Y.; Shim, H. K. *Chem. Eur. J.* **2010,** *16*, 3743–3752; (c) Zhang, M.; Fan, H.; Guo, X.; Yang, Y.; Wang, S.; Zhang, Z. G.; Zhang, J.; Zhan, X.; Li, Y. *Polym. Sci. Part A: Polym. Chem.* **2011,** *49*, 2746–2754.

12 Sahu, D.; Patra, D.; Padhy, H.; Huang, J. H.; Chu, C. W.; Lin, H. C. *J. Polym. Sci. Part A: Polym. Chem.* **2010,** *48*, 6182−6192.

13 (a) Piot, L.; Palma, C. A.; Pallas, A. L.; Prato, M.; Szekrényes, Z.; Kamarás, K.; Bonifazi, D.; Samorì, P. *Adv. Funct. Mater.* **2009,** *19*, 1207–1214; (b) Kuo, C. Y.; Su, M. S.; Ku, C. S.; Wang, S. M.; Lee, H. Y.; Wei, K. H. *J. Mater. Chem.* **2011,** *21*, 11605–11612.

14 (a) Delbosc, N.; Reynes, M.; Dautel, O. J.; Wantz, G.; Porte, J. P. L.; Moreau, J. J. E. *Chem. Mater.* **2010,** *22*, 5258–5270; (b) Liu, Y.; Xiao, S.; Li, H.; Liu, H.; Lu, F.; Zhaung, J.; Zhu, D. *J. Phys. Chem. B.* **2004,** *108*, 6256–6260.

15 Li, Z.; Pei, J.; Li, Y.; Xu, B.; Deng, M.; Liu, Z.; Li, H.; Lu, H.; Li, Q.; Tian, W. *J. Phys. Chem. C* **2010,** *114*, 18270–18278.

16 (a) Padhy, H; Sahu, D.; Patra, D.; Pola.M. K.; Huang, J. H.; Chu, C. W.; Wei, K. H.; Lin, H. C. *J. Polym. Sci. Part A: Polym. Chem.* **2011,** *49*, 3417–3425; (b) Padhy, H.; Huang, J. H.; Sahu, D.; Patra, D.; Kekuda, D.; Chu, C. W.; Lin, H. C. *J. Polym. Sci. Part A: Polym. Chem.* **2010,** 4823–4834.

17 Wu, J. S.; Cheng, Y. J.; Dubosc, M.; Hsieh, C. H.; Chang, C. Y.; Hsu, C. S. *Chem. Commun.* **2010,** *46*, 3259–3261.

18 Zhang, Y.; Hau, S. K.; Yip, H. L.; Sun, Y.; Action, O.; Jen, A. K. Y. *Chem. Mater.* **2010,** *22*, 2696–2698.

19 Kleinhenz, N.; Yang, L.; Zhou, H.; Price, S. C.; You, W. *Macromolecules* **2011,** *44*, 872–877.

20 (a) Li, Y.; Xu, B.; Li, H.; Cheng, W.; Xue, L.; Chen, F.; Lu, H.; Tian, W. *J. Phys. Chem. C* **2011,** *115*, 2386–2397; (b) Li, Y.; Li, Z.; Wang, C.; Li, H.; Lu, H.; Xu, B.; Tian, W. *J. Polym. Sci. Part A: Polym. Chem.* **2010,** *48*, 2765–2776.